In-vitro and clinical evaluation of transurethral laser-induced prostatectomy (TULIP)

van Swol, Christiaan, Verdaasdonck, Rudolf, Mooibroek, Jaap, Boon, Tom

Christiaan F. P. van Swol, Rudolf M. Verdaasdonck, Jaap Mooibroek, Tom A. Boon, "In-vitro and clinical evaluation of transurethral laser-induced prostatectomy (TULIP)," Proc. SPIE 1879, Lasers in Urology, Gynecology, and General Surgery, (28 May 1993); doi: 10.1117/12.146222

SPIE.

Event: OE/LASE'93: Optics, Electro-Optics, and Laser Applications in Scienceand Engineering, 1993, Los Angeles, CA, United States

In vitro and clinical evaluation of transurethral laser induced prostatectomy (TULIP)

Christiaan FP van Swol, Rudolf M Verdaasdonk, Jaap Mooibroek and Tom A Boon

University Hospital Utrecht, Dept. of Urology, Dept. of Radiotherapy and Laser Center, P.O. Box 85500, Utrecht, the Netherlands

ABSTRACT

Transurethral ultrasound-guided laser induced prostatectomy (TULIP) is a recent development in the treatment of benign prostatic hyperplasia. The system is based upon Nd:YAG laser irradiation delivered by a right angled fiber. The dosimetry used in a clinical situation is mostly based upon animal studies.

In this study, the light and temperature distribution in the prostate during Nd:YAG laser irradiation were modeled using Monte Carlo and finite differences theory. The results of this model were compared with *in vitro* experiments. The influence of the different parameters involved, e.g., the scanning speed and the power of the laser beam, were evaluated. Initial results show the temperature distribution and thus the therapeutic effect of the TULIP procedure.

Until now 36 patients have been treated successfully. The mean in-hospital time was somewhat shorter than for a TURP treatment while the results were comparable. These treatments, however, show the need for a better understanding of the mechanisms involved.

Modeling and subsequent *in vitro* and *in vivo* measurements might improve the understanding and safe and successful application of prostate treatment using laser based systems.

1. INTRODUCTION

Transurethral laser coagulation of the prostate as an alternative treatment for benign prostatic hyperplasia is a promising new adjuvant to transurethral resection of the prostate. The dosimetry used in these therapies is based upon animal experiments[1] and adjusted according to the results of the initial patient treatments. In this study, a model is presented which calculates the dynamic temperature distribution in the prostate induced by transurethrally delivered Nd:YAG laser light. The study focuses on the TULIP method[2], used with patient treatments in our hospital, but can easily be extended to other methods using a side firing fiber.[3,4]

2. DEVICE DESCRIPTION

The approach used in our hospital employs a device with the acronym TULIP, which stands for Transurethral Ultrasound-guided Laser Induced Prostatectomy.[5,6] The equipment consists of three components: the Nd:YAG laser, the ultrasound console and the combined ultrasound laser probe (the delivery system). The probe consists of a rigid steel sheath that houses a 600 μm fiber and a window for laser light delivery as well as a transducer for ultrasound imaging. A disposable sleeve is fitted around the probe. During the operative procedure a non-compliant balloon at the distal end of the

0-8194-1106-X/93/$4.00

sleeve is inflated inside the urethra at the prostate level. The balloon contains a small amount of water which allows efficient coupling of the ultrasound waves and the laser light into the tissue. The balloon has more advantages: it causes the optical properties of the prostate to change in such a way that the light penetrates deeper into the tissue, the temperature at its surface is clamped at 100 °C and it assures a constant distance of the fiber to the tissue. Within the inflated balloon the probe can be rotated over 360° and moved freely 5 cm along the longitudinal axis. This allows irradiation of the prostate from the bladder neck up to the apex using the ultrasound scanner for anatomical guidance. Three stages of tissue effect caused by the generated heat can be distinguished: the tissue is blanched directly after the treatment, next a larger volume of tissue that is heated indirectly by heat diffusion becomes necrotic and finally the tissue responds with a healing reaction.

The dosimetry we used during patient treatments was 40 Watts power to tissue and a pull rate of the probe in the balloon of approximately 0.75 mm/s.

3. PATIENT TREATMENTS

Up till 36 patients have been treated using the TULIP system. The median follow up is 5.6 months (range 2-11 months); mean age 66 (46-83) year; mean prostate weight 30 (20-60) grams. The subjective voiding complaints were evaluated using the WHOPSS symptom and bother score pre- and 6 months post-operative. The scores of the first 10 patients are:

Patient #	Symptom score		Bother Score	
	Pre	Post	Pre	Post
1	16	2	23	2
2	20	8	16	8
3	21	15	14	11
4	22	7	15	1
5	24	8	20	2
6	21	10	11	7
7	5	3	7	4
8	26	4	17	13
9	20	5	5	0
10	17	2	16	1

Table 1. Symptom and bother scores pre- and post-TULIP

Uroflow, too, improved significantly: both Q_{max} and $Q_{average}$ showed a significant increase (Q_{max} from 8.7 to 18.4 ml/s and $Q_{average}$ from 3.6 to 9.0 ml/s). The urodynamic results are comparable with a similar group of patients (with regard to the age and prostate weight) treated by TURP. These results are listed below.

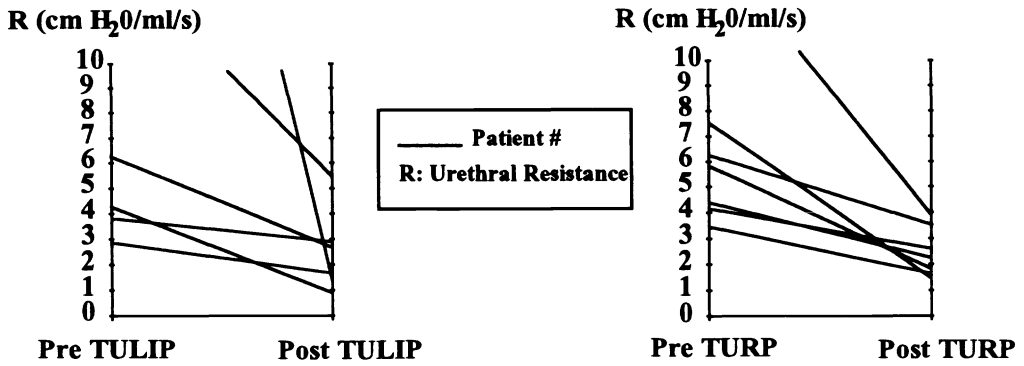

Fig. 1. Urethral resistance pre-and post-TULIP and pre-and post-TURP

These first patient results are promising. Compared to the patients treated with TURP the similarities in change of urethral resistance prove the capability of this method as an alternative with additional benefits (more patient friendly, fewer complications and a shorter hospitalization time).

4. MATERIAL AND METHODS

The laser prostatectomy method as described above was modeled theoretically using a numerical approach and, *in vitro,* experiments were performed.

4.1. Numerical model

The numerical model consists of two parts: an optical and a thermal part, as shown in figure 2.

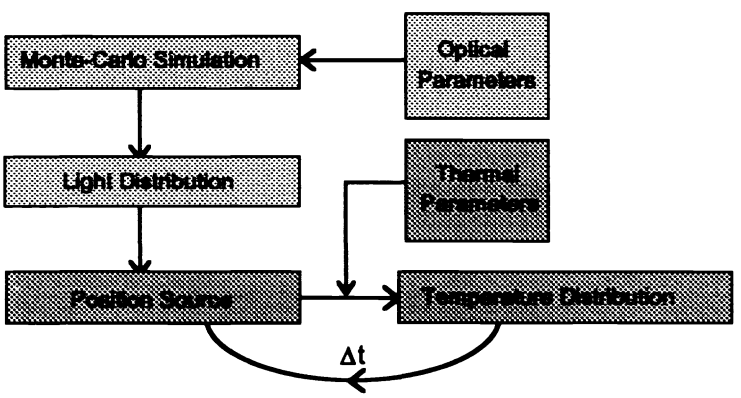

Fig. 2. Lay-out of the numerical model

The light distribution was computed using a Monte Carlo simulation program developed by Keijzer et al.[7] As input for the Monte Carlo program the optical parameters for prostatic tissue at 1064 nm (data taken from Jacques et al.[8]) were used: μ_a=0.37 cm^{-1} and μ'_s=8.2 cm^{-1}. Using the light distribution the generated heat due to absorption was calculated. The thermal properties of the tissue were taken from Mooibroek et al.[9]: $C_{p,tissue}$=3600 $J.Kg^{-1}.K^{-1}$ and k_{tissue}=0.5 $W.m^{-1}$. Consequently, the dynamic temperature distribution in the tissue was calculated using the method of finite differences.[9] The geometry

was simplified by assuming it to be planar. The optical and thermal parameters were assumed to be independent of temperature. The tissue model, as depicted in figure 3, was divided in 50x50x100 cubic elements with individual selectable thermal parameters. Thermal conditions at each of the six boundary planes could be defined independently as isothermal, adiabatic or ascribed by a heat transfer coefficient. The temperature in a particular element at a each time step $T=t+\Delta t$ was calculated from the temperature at T=t at that location and its six neighboring locations. The algorithm used has proved to be unconditionally stable for an arbitrary time step.

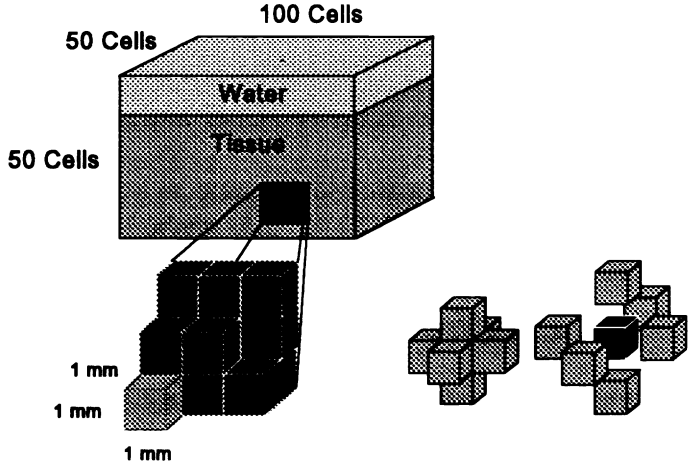

Fig. 3. Model geometry of the tissue phantom used

At the time T=0 the heat source was activated in the tissue model and consequently with every time step moved forward with a particular speed.

In the numerical model the geometry and the dimensions were chosen to simulate the clinical situation as much as possible. The urethra was represented by a five millimeter layer of water on top of the tissue.

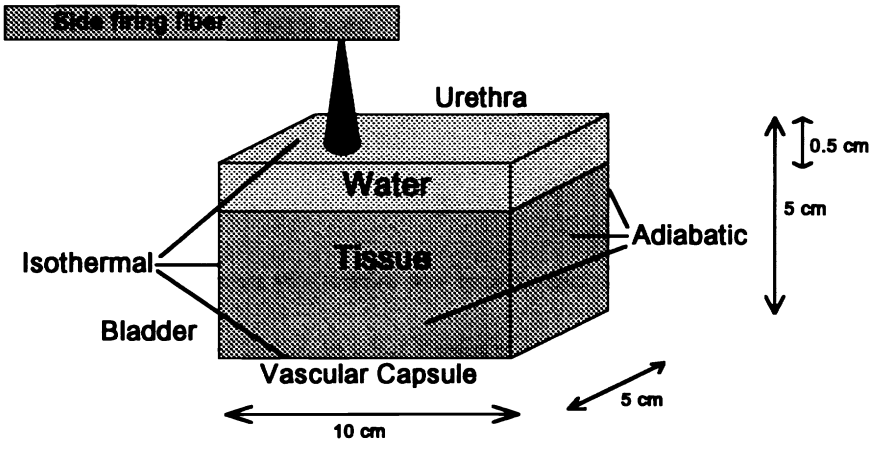

Fig. 4. Dimensions and boundary conditions of the phantom model used

As boundary conditions the planes at the side of the bladder, the vascular capsule and the urethra were assumed isothermal, the other planes were assumed adiabatic. The diameter of the beam used was 3 mm at the water tissue interface. The power of the laser light was scaled in the results afterwards to see the effect of the different parameters involved. At the start, the heat source was situated in the center of the left side of the phantom model. The source remained there for five seconds and then started moving with either 0.5, 1 or 2 mm/sec to the right. The results were stored every 5 seconds. From the calculated three dimensional array either a transversal or an axial plane was taken for graphical representation (figure 5). A series of graphs each five seconds apart was displayed as a video sequence.

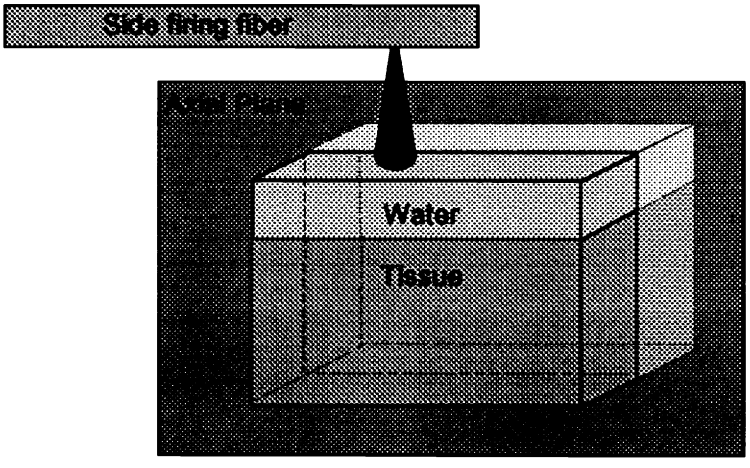

Fig. 5. Two dimensional axial view plane of the calculated distribution

4.2. Experimental model

An optical technique, presented by Verdaasdonk et al.[10] was used to verify the results of the temperature distribution calculated by the numerical model. This technique made it possible to visualize density changes induced by temperature gradients. The experimental set up is shown in figure 6.

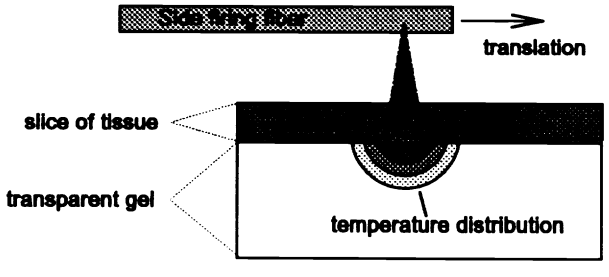

Fig. 6. Experimental set up to visualize temperature distributions in tissue

The geometrical set up and the color coding of the temperature distribution were matched with the numerical model. A slice of tissue was positioned on top of polyacrylamide gel (consisting of 80% water) that has the same thermal properties as the tissue. Gel was chosen because the medium in which

the temperature distribution is to be visualized must be transparent for white light. The tissue used was aortic tissue, as it was rather easy to obtain and it was assumed to have comparable optical properties. A 600 μm fiber was mounted on a mechanical translator and could be freely moved 5 cm in one direction. The tissue was irradiated with different power settings (10-40 Watts) and the translation speed was varied from 0.5 to 2 mm/sec. The thickness of the slice of tissue was chosen in such a way that all optical interaction would take place in this slice. The thus created heat distribution, extended into the gel and became visible color coded. The whole configuration was submerged in water. The created images were recorded with a video camera.

5. RESULTS

5.1. Numerical model

The results after 20 and 60 seconds are displayed in the figures below. Unfortunately the black and white figures give a poor representation of the original color ones. The size of all the frames is 5x10 cm. The frames in the top row represent the axial plane exactly through the middle of the model and through the center of the laser beam. The frames in the middle row are at 5 mm distance from the center and in the lower row the frames are at 10 mm from the center.

Fig. 7. Results of the numerical model (axial plane) after 20 and 60 seconds

Fig. 8. Results of the numerical model (axial plane), magnification of right part of figure 7

The only parameter changed in figure 7 is the scanning speed: the left row is at 0.5 mm/sec, the middle row is at 1.0 mm/sec and the right row is at 2.0 mm/sec. The uniformity of the temperature build-up, created in the first five seconds, remains the same for the slowest scanning speed, but at a higher speed the distribution becomes less uniform. The heat penetrates deeper into the tissue with slower scanning

speeds and so the associated coagulation depth becomes higher.

5.2. Experimental model

In the following figure a black and white representation of a typical example of an image created by the experimental model is shown.

Fig. 9. Image created by the experimental model.

For comparison with the numerical model (see figure 8) similar parameters were used. The initial delay after switching on the laser, as mentioned before, seemed of major influence on the uniformity of the temperature distribution created. Varying the scanning speed determined whether the distribution would stay uniform and affect the penetration of the heat into the tissue. The combination of too high power density with too slow scanning speed caused unpredictable 'popcorn', carbonization and ablation of the tissue.

6. DISCUSSION

The initial results from the experimental *in vitro* model show that the trends predicted by the numerical model are in good agreement. Although the modeling has been focused on the TULIP system, as this is the system currently used in our hospital, both the optical and the thermal model can easily be adapted for other side firing fiber modalities. Predicting the effect of, e.g., cooling by blood vessels or a specific geometry of the prostate using our model will contribute to a more scientifically based dosimetry and will also allow to adapt dosimetry from patient to patient.

At the moment, besides the TULIP system other laser therapies based upon a side firing fiber combined with a Nd:YAG laser are used to perform prostatectomy. The way of using these fiber devices, however, is different. The fiber can be used in contact with the tissue or not and it can be dragged through the prostate or fixed at one piace. The powers used differ from 10 to 60 Watts. The mechanism of action behind these modalities is not well understood. Modeling different treatments of BPH using a Nd:YAG laser will contribute to provide a more fundamental base to optimize and safeguide.

Combining the numerical model above and a rate process damage model together it should be possible to predict the extent of laser-induced thermal damage and thus the success of the therapy. The

Henriques equation[11] provides a relationship between the temperature response of tissue to heating and any resulting thermal damage. This damage model assumes that thermal denaturation is a rate process.

During heating the optical properties, μ_a and μ'_s, of the tissue change.[12] These changes influence the Monte Carlo simulation and result in a different light source (and associated heat source). The thermal parameters, k and c, which are used as an input for the temperature distribution calculation, will also change.[13] The numerical model can be improved by feeding these changes back into the model shown in figure 2, resulting in figure 10.

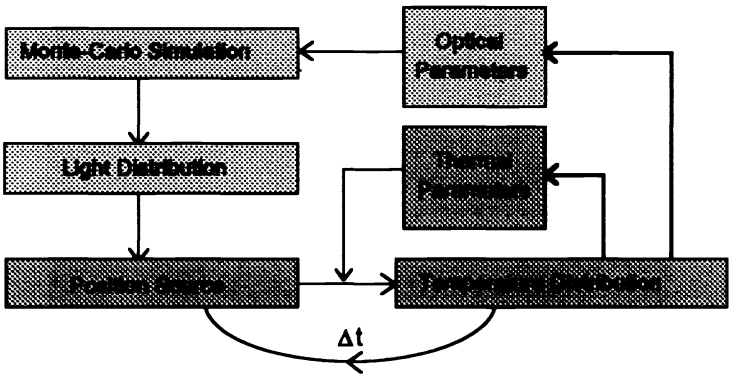

Fig. 10. Feed back of the change in tissue properties

Another change which has to be considered during laser irradiation of tissue is the 'popcorn' effect[14]. The subsurface tissue water is heated above ambient pressure boiling temperature but is prevented from escaping out of the tissue. At a sudden moment, the vapor pressure exceeds tissue resistance and vapor escapes through an explosion to the surface (causing the typical 'pop' sound). Structural changes in the tissue and carbonization and ablation following 'popcorn' make the coagulation process uncontrollable.

7. CONCLUSION

Clinical application of the TULIP system seems a safe treatment for benign prostatic hyperplasia with promising results. Modeling and subsequent *in vitro* experiments are useful for the understanding of the mechanism behind laser prostatectomy and can contribute to a safe and successful application.

8. REFERENCES

1. Kandel LB, Lloyd HH, McCullough DL, Woodruff RD, Dyer RB, "Transurethral laser prostatectomy in the canine model", Lasers Surg. Med., Vol. 12, pp. 33-42, 1992.
2. Roth RA, Aretz HT, "Transurethral Ultrasound-guided Laser-induced Prostatectomy (TULIP procedure): a canine feasibility study", J. Urol., Vol. 146, pp. 1128-1135, 1991.
3. Costello AJ, Bowsher WG, Bolton DM, Braslis KG, Burt J, "Laser ablation of the prostate in patients with benign prostatic hypertrophy", Br. J. Urol., Vol. 69, pp. 603-608, 1992.
4. Johnson DE, Levinson AK, Greskovich FJ, Cromeens DM, Ro JY, Costello AJ, Wishnow KI, "Transurethral laser prostatectomy using a right-angle delivery system", Lasers in urology, laparoscopy

and general surgery, Watson MW, Steiner RW, Pietrafitta JJ, ed., SPIE, Bellingham, Vol. 1421, pp. 36-41, 1991.
5. McCullough DL, "This month in investigative urology: transurethral laser treatment of benign prostatic hyperplasia", J Urol., Vol. 146, pp. 1127-1128, 1991.
6. Babayan RK, Roth RA, "Transurethral Ultrasound-guided laser induced prostatectomy", Lasers in urology, laparoscopy and general surgery. Watson MW, Steiner RW, Pietrafitta JJ, ed., SPIE, Bellingham, Vol. 1421, pp. 42-44, 1991.
7. Keijzer M, Jacques SL, Prahl SA, Welch AJ, "Light distributions in artery tissue: Monte Carlo simulations for finite-diameter laser beams", Lasers Surg. Med., Vol. 9, pp. 148-154, 1989.
8. Jacques LJ, Thomsen S, Schwartz J, Motamedi M, Rastegar S, Mannonen I, "Comparing tissue optics and coagulation for a diode laser (805 nm) versus the Nd:YAG laser (1064 nm)", Lasers Surg. Med., Suppl. 4, pp. 5, 1992.
9. Mooibroek J, Lagendijk JJW, "A fast and simple algorithm for the calculation of convective heat transfer by large vessels in three-dimensional inhomogeneous tissues", IEEE Trans. Biomed. Eng., Vol. 38, pp. 490-501, 1991.
10. Verdaasdonk RM, Borst C, "Optical technique for color imaging of temperature", Laser tissue interaction III, Jacques LJ, ed., SPIE, Bellingham, 1993 (in press).
11. Henriques FC, "Studies of thermal injury", Arch. Pathol., Vol. 43, pp. 489-502, 1947.
12. Splinter S, Svenson RH, Littmann L, Tuntelder JR, Chuang CH, Tatsis P, Thompson M, "Optical properties of normal, diseased and laser photocoagulated myocardium at the Nd:YAG wavelength", Lasers Surg. Med., Vol. 11, pp. 117-124, 1991.
13. Valvano JW, Allen JT, Bowman HF, "The simultaneous measurement of thermal conductivity, thermal diffusivity, and perfusion in small volumes op tissue", ASME J. Biomed. Eng., Vol. 106, pp. 192-197, 1984.
14. Verdaasdonk RM, Borst C, van Gemert MJC, "Explosive onset of continuous wave laser ablation", Phys. Med. Biol., Vol. 35, pp. 1129-1144, 1990.